Chalcogenide Letters Vol. 22, No. 4, April 2025, p. 331 - 339

Enhanced performance of tin sulfide thin-film solar cells via silicon substrate integration: a combined experimental and simulation study

O. Mekhbi [a], K. Kamli [b,*], Z. Hadef [b], O. Kamli [c], M. Bouatrous [d], N. Houaidji [e], L. Zighed [h]

[a] *Department of Technology, Faculty of Technology, University 20 August 1955, BP 26, 21000, Algeria*
[b] *Department of Physics, Faculty of Sciences, University 20 August 1955, BP 26, 21000, Algeria*
[c] *Department of mining and geology, Faculty of Technology, Bejaia University, 06000, Algeria*
[d] *Laboratory of condensed matter physics and nanomaterials, Jijel University, 18000, Algeria*
[e] *Laboratoire de physic-chimie des materiaux, Université Chadli Bendjedid, El-Taref*
[h] *Department of Petrochemistry and Process Engineering, 20 Aout 1955 University of Skikda, Algeria*

This work presents a hybrid study that employs Ultrasonic Spray method for the deposition of SnS absorber films and SCAPS-1D simulation method for the analysis of various solar cell topologies. Different deposition times have been employed to optimize structural, optics, and electrical properties. To evaluate their potential as absorber layers for solar cells, the films were analyzed by using X-ray diffraction (XRD), Scanning Electron Microscopy (SEM), and tested for electrical performance. Complementary numerical simulations were carried out with SCAPS-1D in modeling ZnO:Al/i-ZnO/SnS_2/SnS solar cell structures. Results showed that optimized SnS thickness of 2.5 µm and high carrier density improve the performance of the devices and with a maximum of 6.37% PCE when integrated with silicon substrates.

(Received January 17, 2025; Accepted April 22, 2025)

Keywords: Solar cell, Ultrasonic spray method, SCAPS-1D, SnS absorber, Silicon

1. Introduction

The continuous push for renewable energy sources has considerably upped the research in improving solar cell technologies. Among a number of different materials, tin sulfide (SnS) is a potential candidate as absorber layer for solar cells because of its abundance on earth, nontoxic nature, and proper optoelectronic properties [1, 2]. SnS consists of a direct bandgap of approximately 1.3–1.4 eV with relatively high optical absorption coefficients; however, most SnS-based solar cell devices do not perform up to their expected potential [1-3]. This fact further necessitates that its properties be thoroughly understood and how it behaves under different experimental and simulated conditions.

SnS layers were fabricated using USP (Ultrasonic Spray Pyrolysis), a technique known to balance efficiency, cost-effectiveness, and scalability, making it a promising candidate for large-scale production [1-5]. The experimental study specifically varied the deposition parameters to enhance the structural performance, optical behaviour, and electrical characteristics of the films. XRD, SEM, and electrical measurements further explored the properties of the material.

In addition to experimentation, simulations were pursued within SCAPS-1D software, an able-bodied method of modeling heterostructures of solar cells [6-9]. All parameters being under control in terms of layer properties, such as thickness, doping density, and temperature, the

* Corresponding author: kenza_kamli@yahoo.fr
https://doi.org/10.15251/CL.2025.224.331

performance of the device could be predicted by researchers with this software and then aligned with experimental data.

Each study attempts to find the best parameters for improving solar cell efficiency, and this surely goes in line with the aim of this study. Experimental and computational methods were combined to assess the ZnO:Al/i-ZnO/SnS_2/SnS solar cell structure's functionality. Notably, their simulations assisted in the assessment of the effects or potential impacts of such parameters as SnS layer thickness and substrate on the essential performance metrices-Voc, Jsc, PCE, among others. Furthermore, the joint use of both the experimental and simulation techniques will finally enable more accurate design and optimization methods related to the SnS solar cells, thus minimizing the current distance between theory and practice.

2. Materials and methodology

2.1. Experimental method

Preparation of SnS precursor solution involved the utilization of a solution comprising a 0.1 M concentration of thiourea ($SC(NH_2)_2$) as the sulfide ion precursor and 0.07 M concentration of tin chloride ($SnCl_2$) (Sigma-Aldrich) as the tin precursor. SnS thin films were deposited onto ordinary glass substrates using an ultrasonic spray pyrolysis system [10]. The substrate temperature was kept constant at 350°C, consistent with previous studies [5, 11, 12]. Using the spray solution, four samples (S_1, S_2, S_3 and S_4) were fabricated under varying deposition durations.

A summary of the experimental parameters is provided in Table 1.

Table 1. Deposition conditions employed in preparing SnS thin films.

Reagents molarity (mol/l)		Temperature (°C)	Time (min)	Volume (ml)	Solvent
$SnCl_2$: $2H_2O$	Thiourea				
0.07	0.1	350	30, 40, 50, 60	100	Methanol

After the deposition of SnS samples in the form of uniform and adherent binary thin films, a set of characterization technics were used to delineate its different properties.

Structural properties of the films were defined using X-ray Diffraction (XRD) (Bruker-AXS D8 diffractometer, CuK_α radiation, $\lambda = 1.541838$ Å). The films' thickness and chemical composition were analyzed via scanning electron microscopy (SEM) (JEOL JSM 6400) combined with energy-dispersive X-ray spectroscopy (EDX). For electrical characterization, the four-point probe technique was employed to measure conductivity and resistivity.

2.1. Simulation methodology and material properties

There has been much solar cell simulation software operating in the market, including GPVDM, SETFOS – FLUXIM, SILVACO ATLAS, SERIIUS and AMPS. Despite these considerations, the simulation software ***SCAPS-1D*** offers a robust and reliable framework for modeling heterostructures, supporting the inclusion of up to seven distinct layers within a single device. Its advanced features enable precise adjustments to layer thickness, doping density, and operating temperature, ensuring alignment with experimental data.

In this study, we employed SCAPS-1D (version 3.3.10) to simulate the Al:ZnO/i:ZnO/SnS_2/SnS solar cell structure shown in Figure 1. The design includes a transparent conductive oxide layer (Al:ZnO), an intrinsic ZnO buffer layer (i:ZnO), an SnS absorber layer, an n-type SnS_2 window layer, and a Mo/glass or Mo/Si substrate, as illustrated in Figure 1.

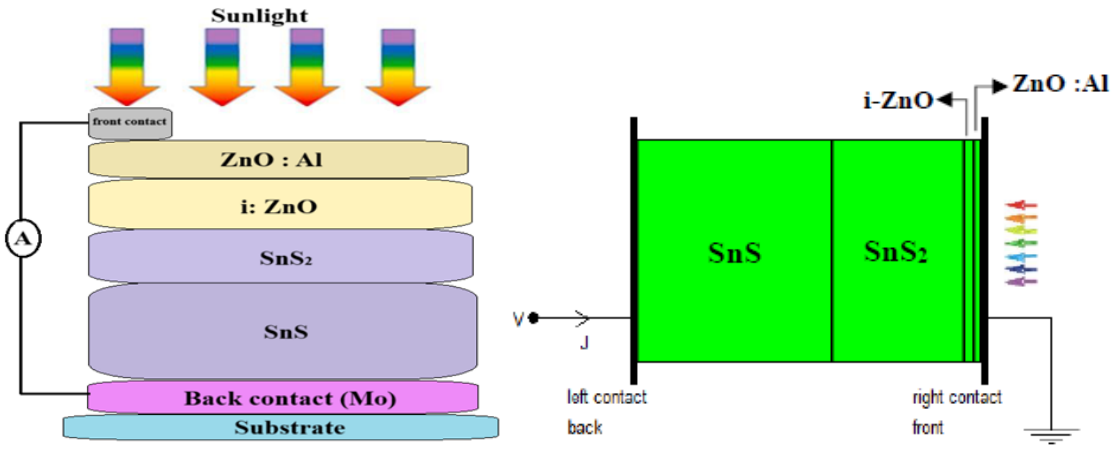

Fig. 1. Structure of the proposed solar cell used for the numerical.

These solar cells considers a transparent, electrically conductive 0.06 μm thick layer of Al:ZnO that is a good ohmic contact with the semiconductor. The material has a wide bandgap of about 3.3 eV. The 0.08 μm thick i:ZnO layer is an intrinsic material supposed to protect the buffer layer during subsequent layer depositions. The SnS_2 with a layer thickness of 1 μm is acting as the buffer layer, while SnS is making up the absorber layer. The Mo layer plays the role of the back contact electrode, collecting holes in the device structure.

Table 2 summarizes the key material properties of the Al:ZnO, i:ZnO, SnS_2, and SnS layers modeled in the simulation.

Table 2. Physical parameters of the proposed solar cell layers.

Parameters	SnS (Absorber Layer)	SnS_2 (Buffer Layer)	i-ZnO (Window Layer)	ZnO:Al (TCO Layer)
Eg (eV)	1.35	1.85	3.3	3.6
Thickness (μm)	1.5 - 2.5	1	0.08	0.06
χ (eV)	4.1	4.26	4.5	4.6
ε_r	13.0	17.7	9	9
N_C (cm^{-3})	1.75×10^{19}	7.32×10^{18}	2.2×10^{18}	2.2×10^{18}
N_V (cm^{-3})	1×10^{19}	1×10^{19}	1.8×10^{19}	1.8×10^{19}
μ_e ($cm^2\ V^{-1}\ s^{-1}$)	130	50	1×10^2	1×10^2
μ_h ($cm^2\ V^{-1}\ s^{-1}$)	57	25	25	25
N_D (cm^{-3})	1.75×10^{18}	9.85×10^{18}	1×10^{18}	1×10^{19}
N_A (cm^{-3})	0	0	0	0
Electron/Hole thermal velocity (cm/s)	10^7	10^7	10^7	10^7
Defect type	Neutral	Neutral	Neutral	Neutral

where: **Eg**: band gap; **χ**: electron affinity; **ε_r**: dielectric permittivity; **N**: effective band states density (for the conduction band **C** and the valence band **V**); **μ**: charge carrier mobility (for e: electrons and h: holes); **N**: defect density (for donors **D** and acceptors **A**).

The one-dimensional simulation tool SCAPS-1D uses Poisson's equations and electron/hole continuity principles to model a solar cell's electronic band structure, charge carrier movement, and recombination dynamics [13, 14]. This approach allows researchers to simulate how these factors influence overall device performance.

Besides, SCAPS 1D offers some select adjustments of the layer thickness, doping density, and temperature for operating purposes and really offers a good match with the experimental data.

3. Results and discussion

3.1. Experimental optimization of the absorbent layer

3.1.1. Thickness films effect on structural properties

The thickness of the films was determined using cross-sectional SEM imaging, as displayed in Figure 2.

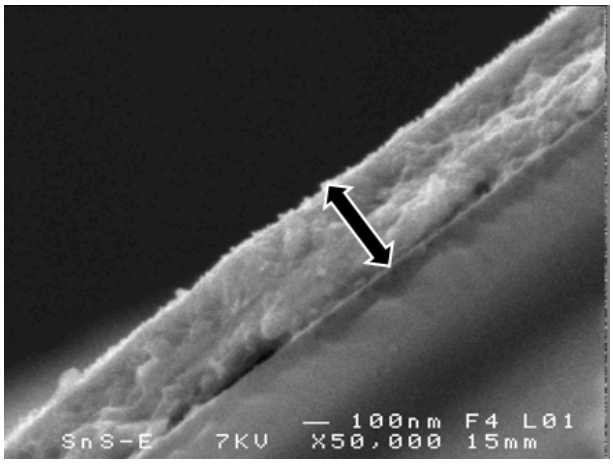

Fig. 2. Crosssectional SEM image of SnS thin film, used for thickness measurement.

Crystallite sizes in the SnS films were estimated from XRD data and later quantified using the Scherrer equation [15].

$$D_{hkl} = \frac{0.9\,\lambda}{\beta_{hkl}\,cos\theta} \tag{1}$$

where: λ is X-ray wavelength, β_{hkl} and θ are the full width at half maxima and the Bragg's diffraction angle of the intense peak of the obtained XRD pattern, respectively.

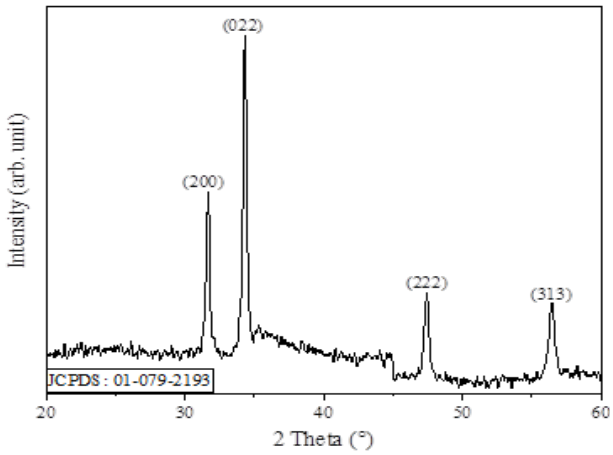

Fig. 3. XRD pattern of the SnS film deposited for 50 min.

Table 2 reports the variation in film thicknesses and some other parameters of SnS thin films deposited for times ranging from 30 to 60 minutes.

Table 2. Films thickness, grain size and atomic percentage of SnS thin films.

Sample	Deposition time (min)	Thickness (µm)	Grain size (nm)	Sn/S (at. %)
S_1	30	1.5	25.47	41.98 / 58.02
S_2	40	2.01	52.01	45.33 / 54.67
S_3	50	2.35	83.21	49.15 / 50.85
S_4	60	2.5	82.72	50.03 / 49.97

According to the Table 2, it can be notice that with rising the deposition time, the films thickness increases and become more stoichiometric. Furthermore, we notice generally an enlargement in the grain size that is a good factor, because this later will reduce the defect (grain boundary) that captures charge carriers [16].

Table 3 presents the different optical and electrical properties of SnS absorber thin films prepared at various deposition times using spray method.

Table 3. Opto-electrical parameters of SnS thin films.

Sample	Band gap (eV)	Resistivity (Ω cm)	Bulk Concentration (cm^{-3})	Type
S_1	1.54	2.23×10^{3}	5.17×10^{15}	P
S_2	1.42	9.56×10^{2}	2.01×10^{16}	P
S_3	1.34	5.16×10^{2}	9.70×10^{18}	P
S_4	1.36	4.03×10^{2}	3.01×10^{19}	P

According to Table 3, the band gap is observed to decrease progressively with thickness increasing, and the samples S3 and S4 exhibit an almost similar Eg of about 1.35 ± 0.01 eV. This value suggests enhanced photon absorption, especially in the visible spectrum. Furthermore, the resistivity decreases significantly from ~10^3 Ω·cm to ~10^2 Ωcm, indicating an improvement in electrical conductivity due to the increasing of the carrier concentration.

These results suggests that the more suitable sample for the solar cell application is S4. Nevertheless, the film S3 with properties close to S4, can be also a good candidate for use in such applications.

The absorber layer thickness and charge carrier density significantly influence the efficiency of thin film solar cells. With increasing absorber layer thickness (before exceeds certain values) [13, 17], the performance of the thin film solar cell increases as absorption of solar photons increases.

3.2. Solar cell simulation

3.2.1. Variation in the open-circuit voltage (Voc)

Figure 4 represents the influence of the thickness variation for an adjusted carrier density on the desired outcome.

The figure shows a color contour map representing the open-circuit voltage (V_{OC}) of a device as a function of **SnS Thickness (µm)** on the x-axis and **Carrier Density (cm^{-3})** on the y-axis.

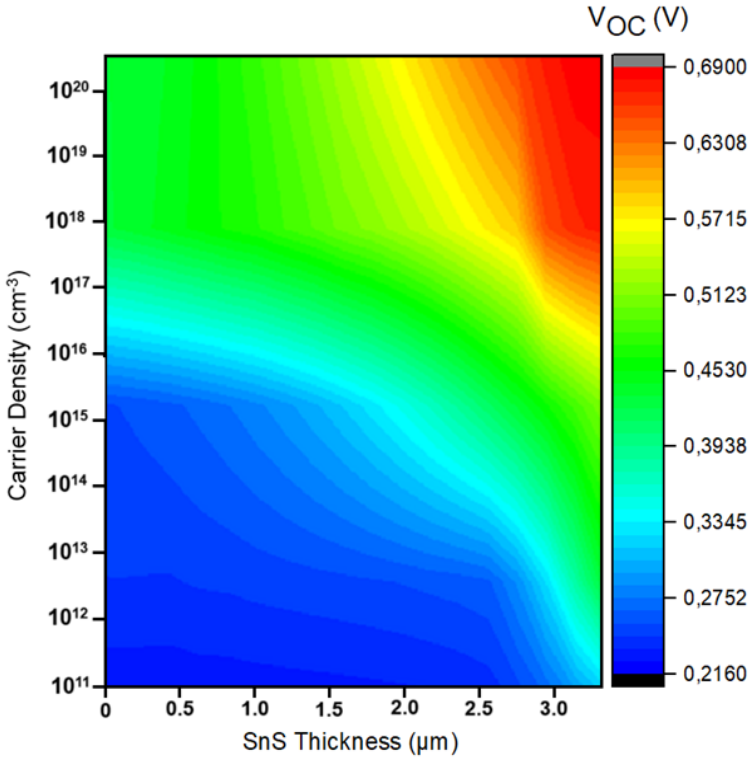

Fig. 4. Variation in the open-circuit voltage (Voc) as a function of the thickness of the SnS absorber and the carrier density in the ZnO:Al/i-ZnO/SnS_2/SnS/Mo structure.

According to figure 4, it can be observed that fluctuations in the open-circuit voltage (Voc) are primarily attributed to variations in the charge carrier density. At low carrier densities (~10^{12} - 10^{15} cm^{-3}), V_{OC} remains low (blue region), irrespective of the SnS absorber layer thickness. By way of carrier density increasing (~10^{17} -10^{20} cm^{-3}), V_{OC} significantly improves, especially for thicker SnS layers. High V_{OC} values (yellow to red) are observed when the carrier density is above 10^{18} cm^{-3} and SnS thickness exceeds ~ 2.5 µm. Furthermore, the augmentation in the hole density induce an increasing in Voc too, which is a result of the higher carrier density [18]. Escape paths also depend on atomic carrier density, as this influences the depletion-region width and minority-carrier life.

As maintained by the obtained results, we can first say that to achieve the highest open-circuit voltage (V_{OC}), the SnS layer thickness should be relatively high (≥ 2.35 µm), and the carrier density should be above 10^{18} cm^{-3}. Lower carrier densities or thinner SnS layers result in reduced V_{OC}, as seen in the blue and green regions.

3.2.2. Current density-voltage (J-V) characteristics of ZnO:Al/i-ZnO/SnS_2/SnS/Mo structure

Figure 5 shows the variation of the current density J as a function of the applied voltage V with varying the SnS thicknesses.

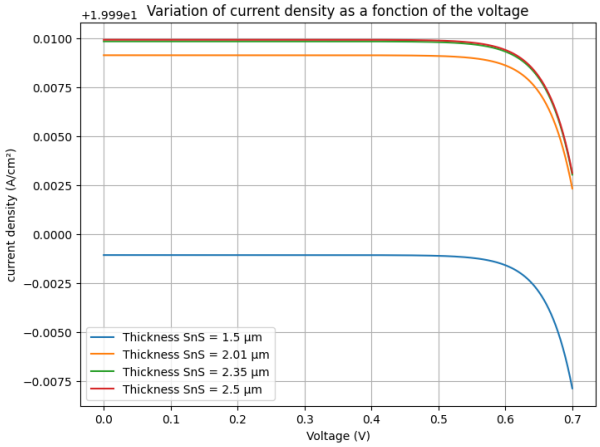

Fig. 5. J-V variation of ZnO:Al/i-ZnO/SnS_2/SnS/Mo structure.

The observed results from this figure confirm the previously obtained results (experimental results). Thicker the SnS absorber layer is, higher and more stable the current density J across the voltage range is obtained. This behavior indicate an improvement in carrier collection and reduction in recombination losses in comparison to the thinner layer.

In other words, increased absorber thickness improves light absorption, resulting in more electron-hole pairs [19]. When the thickness exceeds certain threshold values, it may lead to an increase in recombination losses; however, this effect is not observed within the current range of thicknesses.

3.2.3. Effect of Si substrate on current density-voltage (J-V) characteristics of ZnO:Al/i-ZnO/SnS_2/SnS/Si structure

Figure 6 shows the variation of current density (J) as a function of voltage (V) for a solar cell structure ZnO:Al/i-ZnO/SnS_2/SnS/Si, where silicon (Si) is used as the substrate. The curves correspond to different SnS absorber thicknesses: 1.5 µm, 2.01 µm, 2.35 µm, and 2.5 µm.

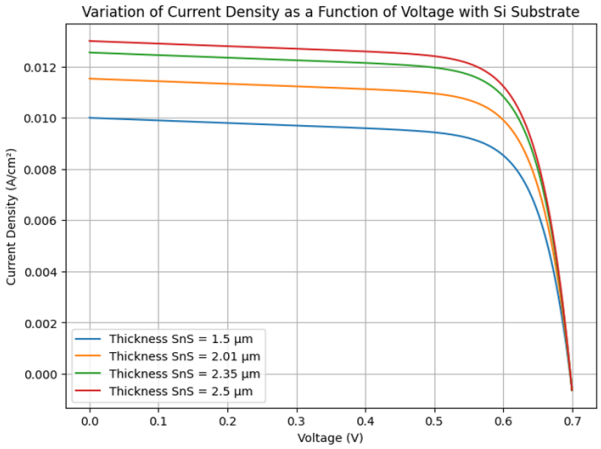

Fig. 6. J-V Curves of ZnO:Al/i-ZnO/SnS_2/SnS/Si structure.

Herein another structure has been used by using Silicon as a substrate, and by varying SnS absorber thickness in order to study their effects on the outcome of the desired solar cell. Our findings suggest that increasing the SnS absorber thickness from 1.5 µm to 2.5 µm significantly boosts current density. This improvement stems from enhanced light absorption in thicker SnS layers, which generates more electron-hole pairs [19]. Furthermore, at low voltages, the current

density closely aligns with the short-circuit current density (Jsc), demonstrating a direct dependence on SnS layer thickness. This later is manifested in better light absorption and charge carrier generation with increasing absorber thickness.

On the other hand, the silicon substrate raises the overall current density [20]. Silicon also allows for better charge collection and lowers the loss of recombination, which is why current density values in systems with silicon substrate are higher than those without it.

3.2.4. Comparison between the best results of the two solar cell structures

By comparing the results obtained from the two solar cell structures, ZnO:Al/i-ZnO/SnS_2/SnS/Mo and ZnO:Al/i-ZnO/SnS_2/SnS/Si, it can be deduced that, despite the good performance of the first structure, the configuration without the silicon substrate exhibits less efficient light absorption and charge carrier collection, resulting in lower overall current density values. Additionally, the second structure's Jsc does, however, improve notably due to the silicon substrate when considering the low voltages (near V=0).

In table 4 we have provide the different calculated characteristics parameters of ZnO:Al/i-ZnO/SnS_2/SnS/Mo and ZnO:Al/i-ZnO/SnS_2/SnS/Si solar cell structures.

Table 4. Numerical parameters of the best results of both solar cell structures.

Cell Structure \ Parameter	SnS Thickness (µm)	Short-Circuit Current Density J_{SC} (mA/cm²)	Open-Circuit Voltage V_{OC} (V)	Fill Factor FF	Power Conversion Efficiency PCE (%)
Without Si Substrate	2.5	10.5	0.7	0.7	5.15
With Si Substrate	2.5	13.0	0.7	0.7	6.37

The silicon substrate plays a crucial role in increasing the performance of the solar cell structure, especially when the absorber thickness of SnS is optimized at 2.5 µm.

Taking silicon as a substrate improves the power conversion efficiency (PCE) from 5.15% up to 6.37%. The observed improvement is primarily driven by an increase in Jsc (short-circuit current density), due to better light absorption and charge collection by the silicon substrate [20-22].

4. Conclusion

This study based on experimental and SCAPS-1D simulations has studied tin sulfide (SnS) as a promising absorber layer of thin-film solar cells. Ultrasonic spray pyrolysis was employed to synthesize SnS thin films and the deposition conditions were optimized to enhance structural integrity, optical response, and electrical conductivity. The experimental results reveal that films 2.5 µm thick had better characteristics-inter-mixing, more carrier concentration, and less resistivity.

The complementary SCAPS-1D based simulations gave extra information concerning the photovoltaic performance of ZnO:Al/i-ZnO/SnS_2/SnS solar cells. From these investigations, it was inferred that the thickness of the absorber layer and carrier concentration in this layer will greatly enhance the power conversion efficiency. Co-integration with silicon also made improvements in performance, increasing PCE from 5.15% to 6.37%.

The combined use of simulation and experimental approaches provided the reconciliation of theoretical predictions and practical findings. This work not only highlights the promise of SnS as an abundant and environmentally friendly solar cell material, but it also establishes a strong concept for the optimization of similar photovoltaic devices through experimental-numerical interfacing. These results provide opportunities for further development at scale for the SnS solar technology.

References

[1] Z. Hadef, K. Kamli, A. Akkari, H. Hadjoudja, N. Turki Kamoun, O. Kamli, A. Djarmoune, F. Ait Merzeg, J Mater Sci: Mater Electron 35(1632), 1 (2024); https://doi.org/10.1007/s10854-024-13370-1

[2] N. Koteeswara Reddy, M. Devika, E. S. R. Gopal, Critical Reviews in Solid State and Materials Sciences, 40 (6), 359 (2015); https://doi.org/10.1080/10408436.2015.1053601

[3] A. Ben Hjal, L. Pezzato, E. Colusso, G. Bragaggia, N. Tormena, N. Trivellin, K. Alouani, M. Dabal'a, K. Brunelli, Journal of Alloys and Compounds 987, 174150 (2024); https://doi.org/10.1016/j.jallcom.2024.174150

[4] R. Schlaf, N.R. Armstrong, B.A. Parkinson, C. Petten-kofer, W. Jaegermann, Surface Science 385 (1), 1 (1997); https://doi.org/10.1016/S0039-6028(97)00066-6

[5] Z. Hadef, K. Kamli, A. Attaf, M. S. Aida, and B. Chouial, Journal of Semiconductors 38 (6), 063001-1 (2017); https://doi.org/10.1088/1674-4926/38/6/063001

[6] M. Burgelman, J. Verschraegen, S. Degrave, P. Nollet, Progress in photovoltaics 12 (2-3), 143 (2004); https://doi.org/10.1002/pip.524

[7] J. Verschraegen, M. Burgelman, Thin Solid Films 515, 6276 (2007); https://doi.org/10.1016/j.tsf.2006.12.049

[8] O. Boultif, B. Zaidi, S. Roguai, A. Mehdaoui, F. Diab, T. Bouarroudj, K. Kamli, Z. Hadef, C. Shekhar, Journal of nano- and electronic physics 15 (2), 02016-1 (2023); https://doi.org/10.21272/jnep.15(2).02016

[9] B. Zaidi, C. Shekhar, K. Kamli, Z. Hadef, S. Belghit, M.S. Ullah, Journal of nano- and electronic physics 12 (1), 01024-1 (2020); https://doi.org/10.21272/jnep.12(1).01024

[10] Z. Hadef, K. Kamli, Materials Today: Proceedings 49, 1079 (2022); https://doi.org/10.1016/j.matpr.2021.09.330

[11] S.M. Ahmed, L.A. Latif, A.KH. Salim, Journal of Basrah Researches (Sciences) 37 (3A), 53 (2011).

[12] K. Kamli, Z. Hadef, B. Chouial, B. Zaidi, B. Hadjoudja, A. Chibani, Surface engineering, 33(8), 567 (2017); https://doi.org/10.1080/02670844.2016.1271593

[13] T. Chargui, F. Lmai, M. AL-Hattab, O. Bajjou, K. Rahmani, Optical Materials 140, 113849 (2023); https://doi.org/10.1016/j.optmat.2023.113849

[14] N. D. Lam, Engineering Research Express, 2 (2), 025033 (2020); https://doi.org/10.1088/2631-8695/ab9716

[15] H. R. Hassan, A. N. Abd, M. J. M. Ali, Chalcogenide Letters 21 (11), 855 (2024); https://doi.org/10.15251/CL.2024.2111.855

[16] K. Kamli, Z. Hadef, O. Kamli, B. Chouial, M. S. Aida, H. Hadjoudja, S. Labiod, Journal of Nano Research 81, 37 (2023); https://doi.org/10.4028/p-DPoy5X

[17] T. Chargui, F. Lmai, et K. Rahmani, Materials Today: Proceedings, S2214785323051040, 2023.

[18] G. T. Koishiyev, J. R. Sites, Solar Energy Materials and Solar Cells 93 (3), 350 (2009); https://doi.org/10.1016/j.solmat.2008.11.015

[19] P. Dubey, Sadanand, B. K. Pandey, D. K. Dwivedi, Optik 266, 169600 (2022); https://doi.org/10.1016/j.ijleo.2022.169600

[20] C. H. Lin, S.P. Hsu, Wei-Chih Hsu, Solar Cells - Silicon Wafer-Based Technologies, InTech, China, 93, 2011.

[21] P. Caño, M. Hinojosa, I. García, R. Beanland, D. F. Marrón, C. M. Ruiz, A. Johnson, I. Rey-Stolle, Solar Energy 230, 925 (2021); https://doi.org/10.1016/j.solener.2021.10.075

[22] S. Boyer-Richard, F. Fan, A. Beck, C. Levallois, K. Tavernier, T. Rohel, R. Bernard, A. Létoublon, C. Cornet, O. Durand, EPJ Photovoltaics 14, 31 (2023); https://doi.org/10.1051/epjpv/2023020